Supplemental Figure 1: In vitro viability data

A

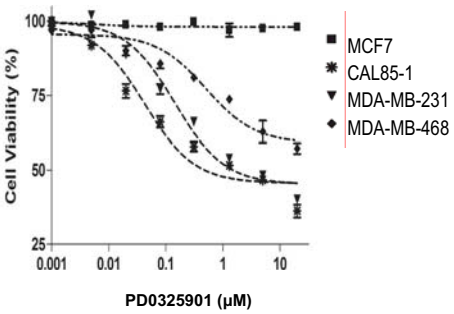

B

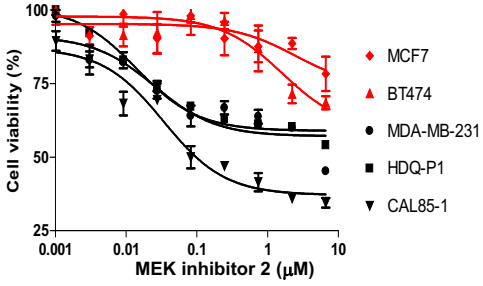

C

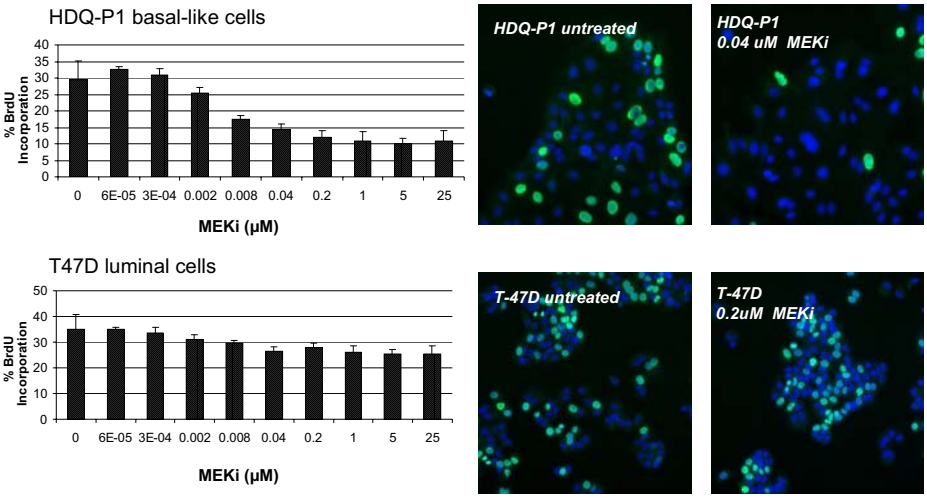

D

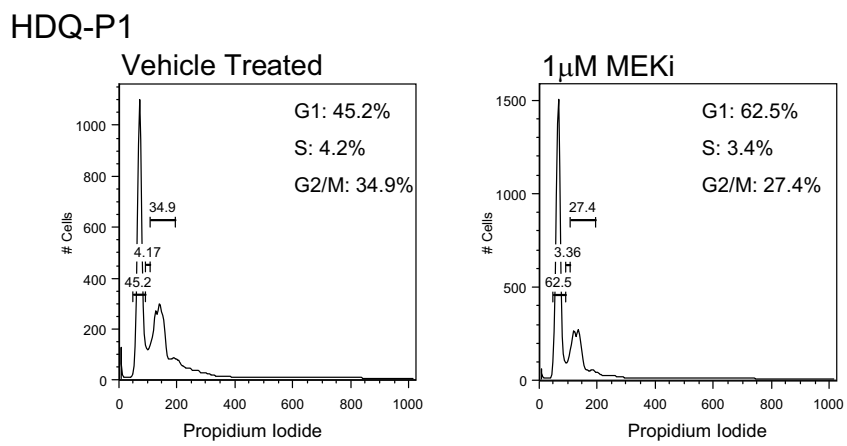

Supplemental Figure 2: PTEN and EGFR in Breast Lines

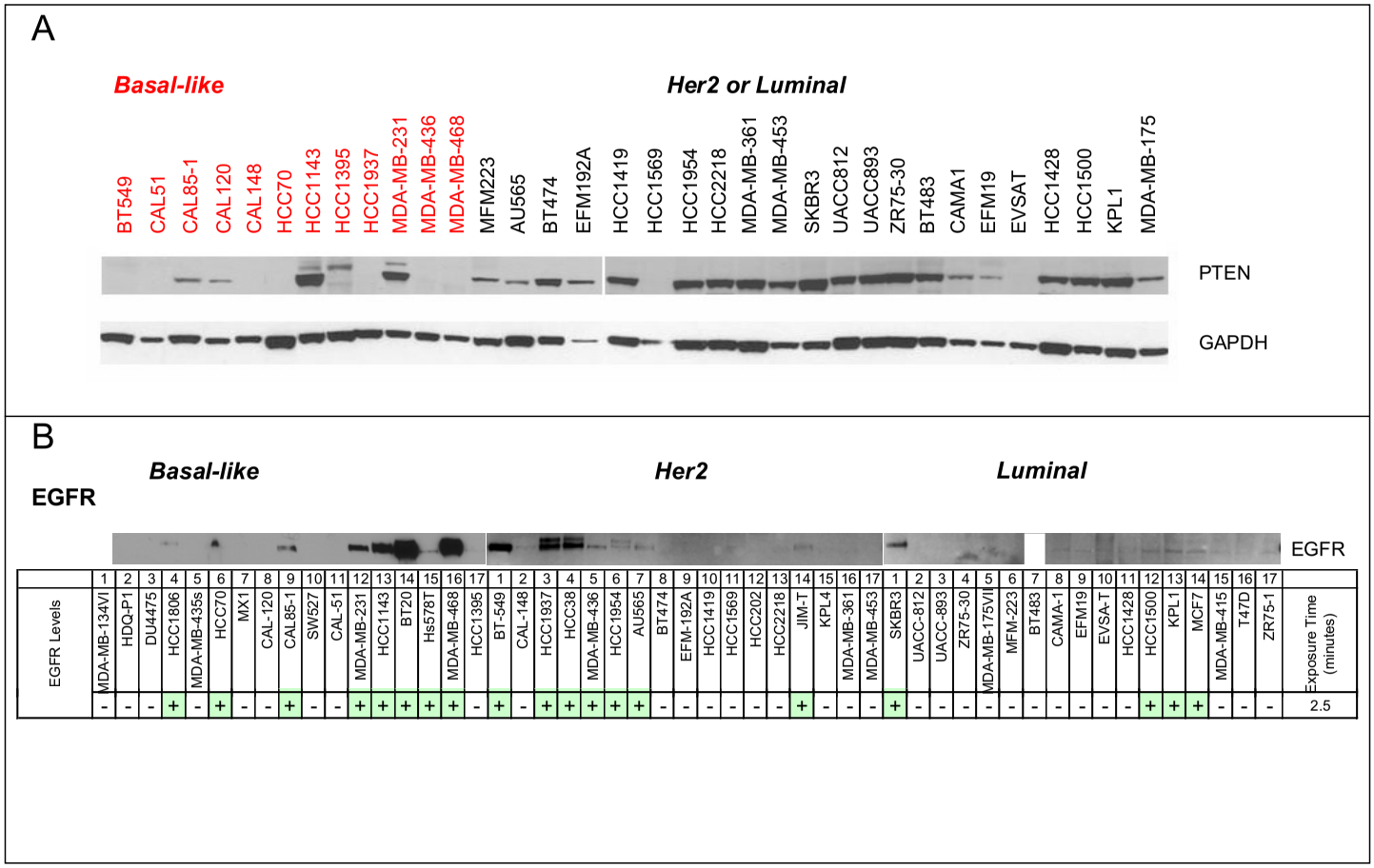

	1	2	3	4	5	6	7	8	9	10	11	12	13	14	15	16	17	1	2	3	4	5	6	7	8	9	10	11	12	13	14	15	16	17	
EGFR Levels	MDA-MB-134VI	HDQ-P1	DU4475	HCC1806	MDA-MB-435s	HCC70	MX1	CAL-120	CAL85-1	SW527	CAL-51	MDA-MB-231	HCC1143	BT20	Hs578T	MDA-MB-468	HCC1395	BT-549	CAL-148	HCC1937	HCC38	MDA-MB-436	HCC1954	AU565	BT474	EFM-192A	HCC1419	HCC1569	HCC202	HCC2218	JIM-T	KPL4	MDA-MB-361	MDA-MB-453	Exposure Time (minutes)
	-	-	-	+	-	+	-	-	+	-	-	+	+	+	+	+	-	+	-	+	+	+	+	+	-	-	-	-	-	-	+	-	-	-	2.5

	1	2	3	4	5	6	7	8	9	10	11	12	13	14	15	16	17	
EGFR Levels	SKBR3	UACC-812	UACC-893	ZR75-30	MDA-MB-175VII	MFM-223	BT483	CAMA-1	EFM19	EVSA-T	HCC1428	HCC1500	KPL1	MCF7	MDA-MB-415	T47D	ZR75-1	Exposure Time (minutes)
	+	-	-	-	-	-	-	-	-	-	-	+	+	+	-	-	-	2.5

Supplemental figure 3: Molecular Classification of Breast Tumor Models

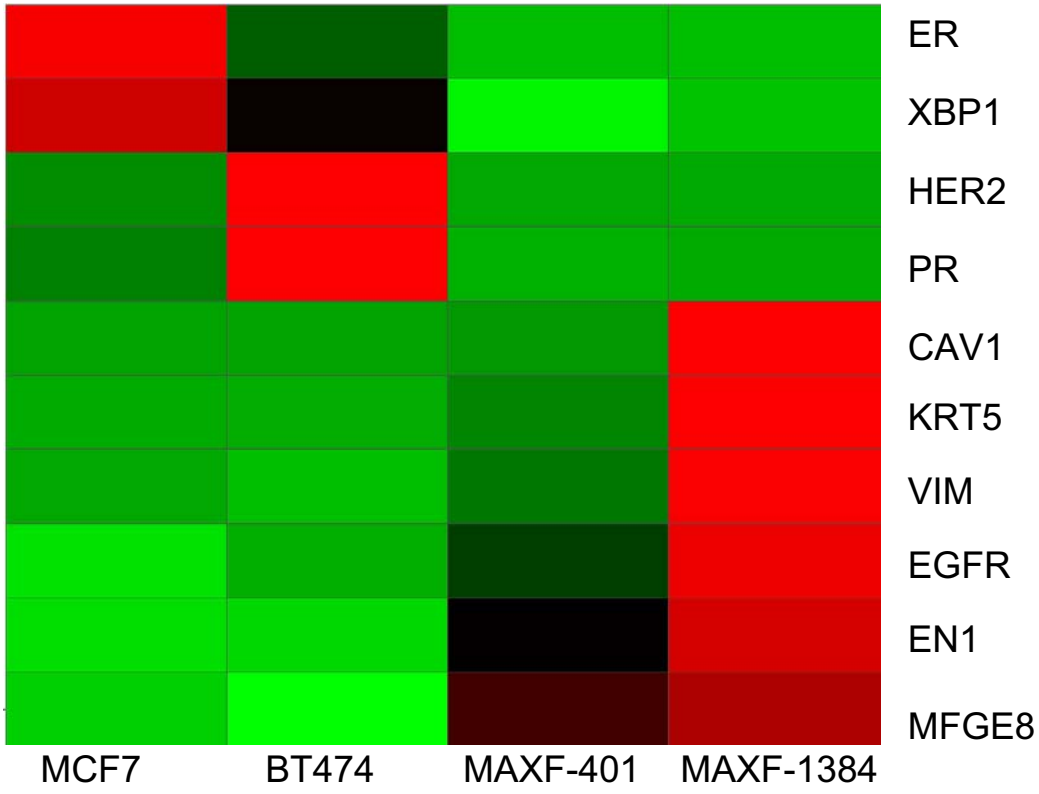

Supplemental figure 4: Pharmacodynamic response to MEK Inhibition in Xenograft Tumors

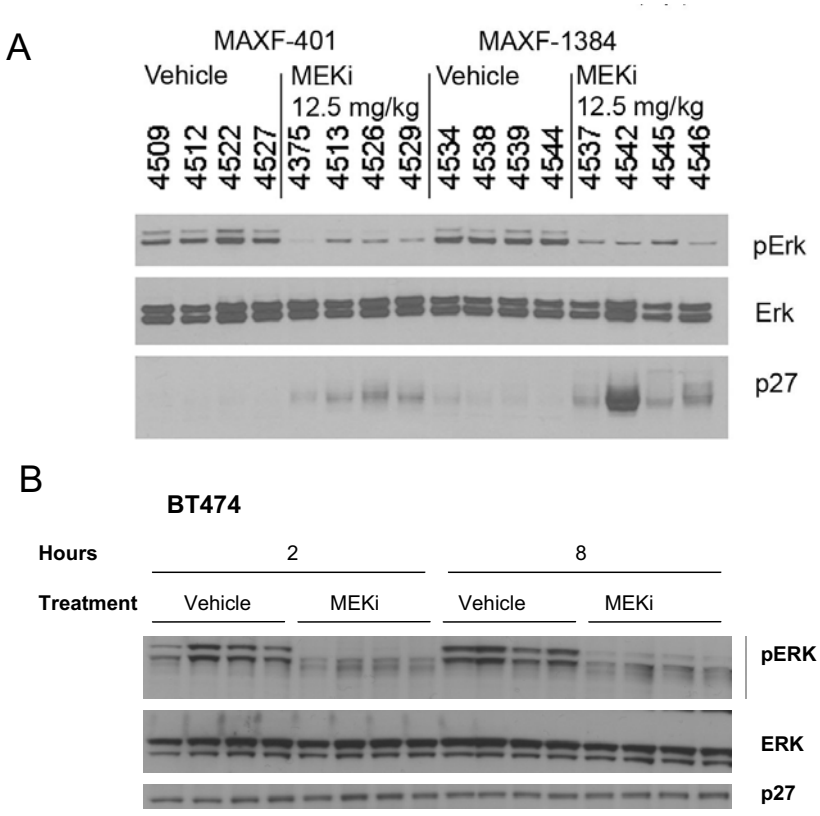

Supplemental Figure 5: 1μM erlotinib treatment downregulates pErk in CAL85-1 but not MDA-MB-231 KRAS mutant cells

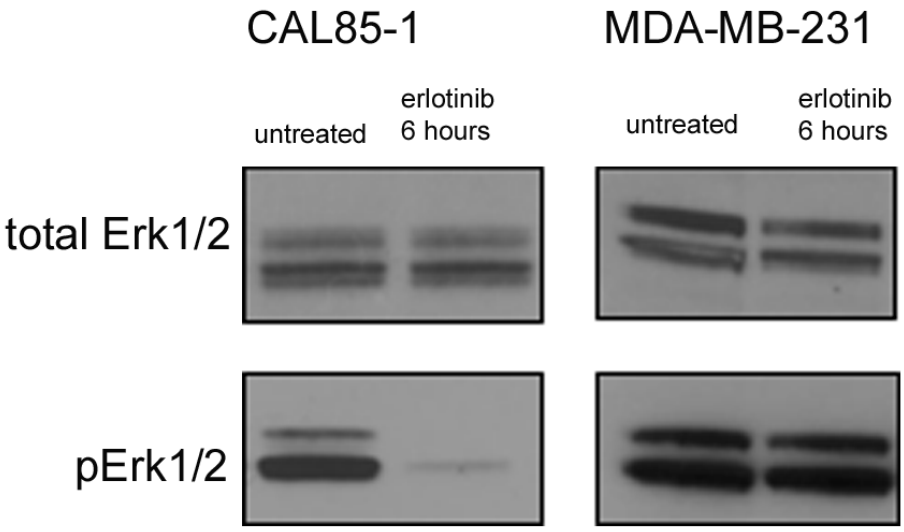

Supplemental figure 6: Quantitation of EGFR and PTEN siRNA Knockdown

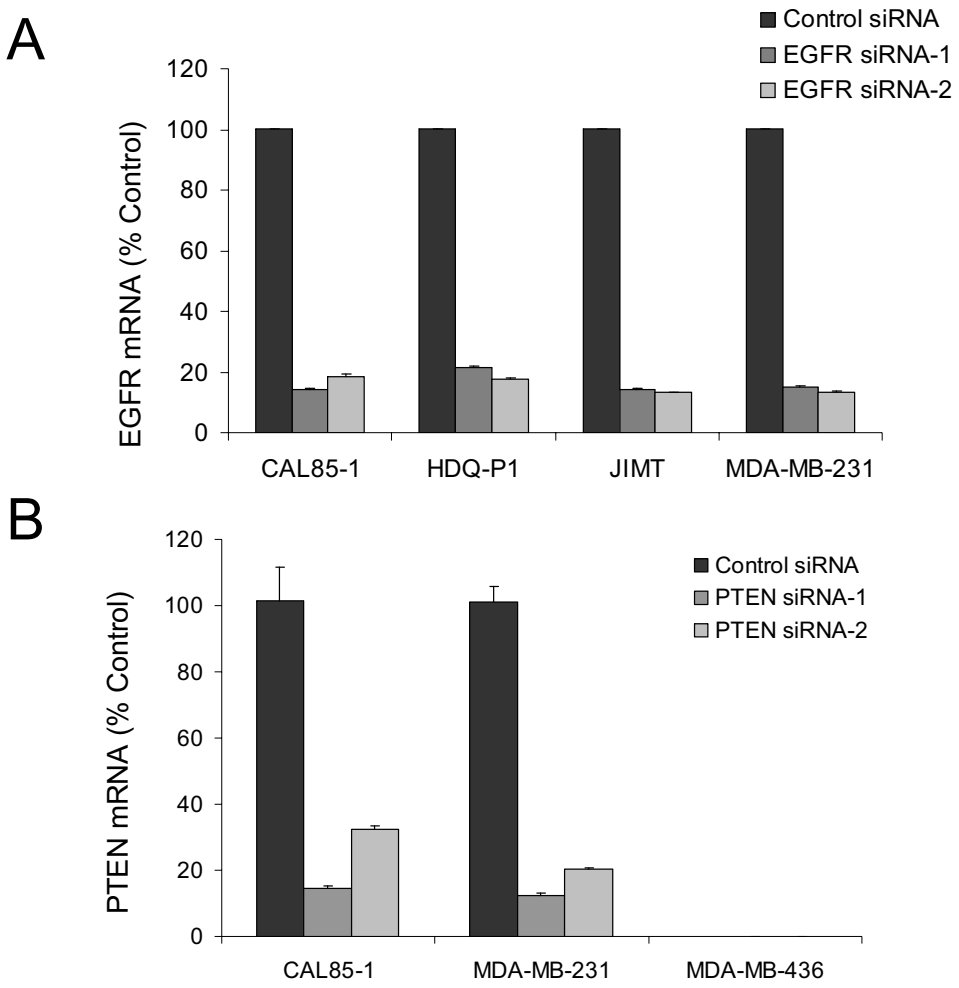

Supplemental figure 7: PTEN siRNA Reduces G1 Arrest in Response to MEK Inhibition

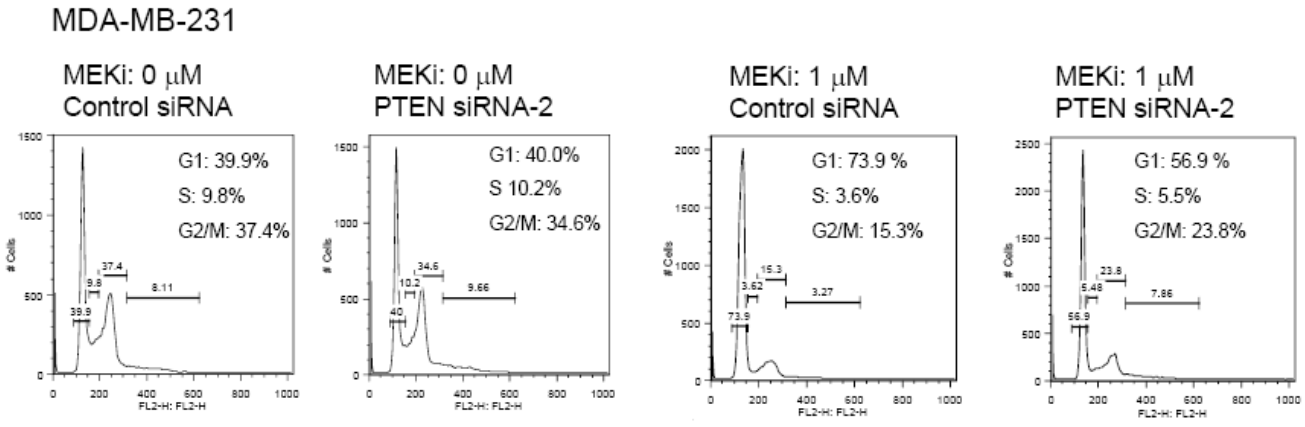

Supplemental figure 8: 1μM MEKi Treatment Increases pAkt(S473) in a Range of Breast Cancer Cell Lines

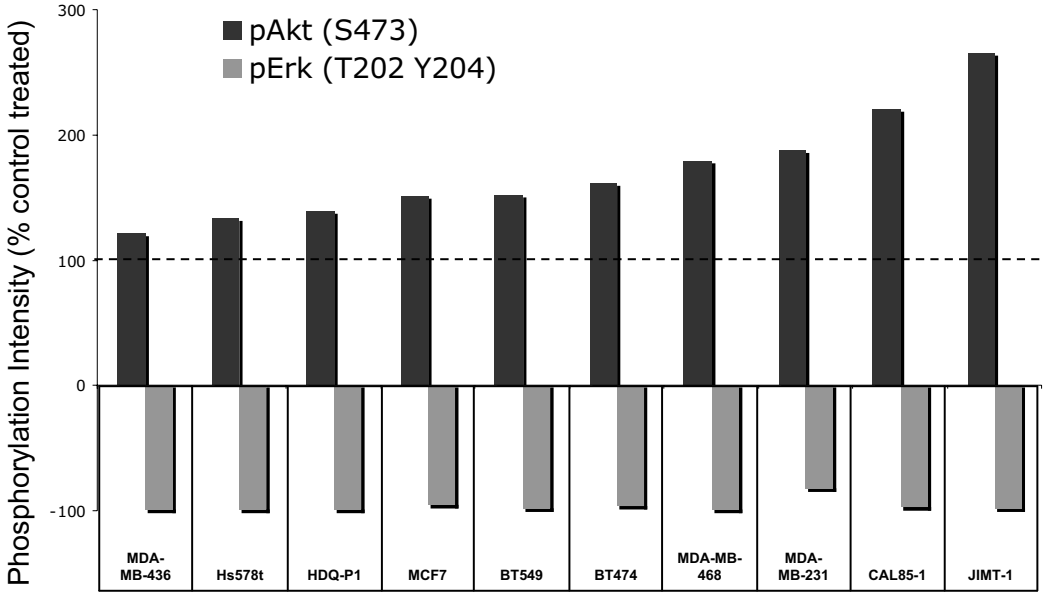

Supplemental figure 9: Cyclin D1 downregulation in response to MEKi, PI3Ki or combination treatment in cell lines that show in vitro synergy (MDA-MB-231 and CAL85-1 data from Figure 5A) or lack of synergy (MCF-7 and JIMT-1). Graphs show quantitation of immunoblot bands using NIH Image J software.

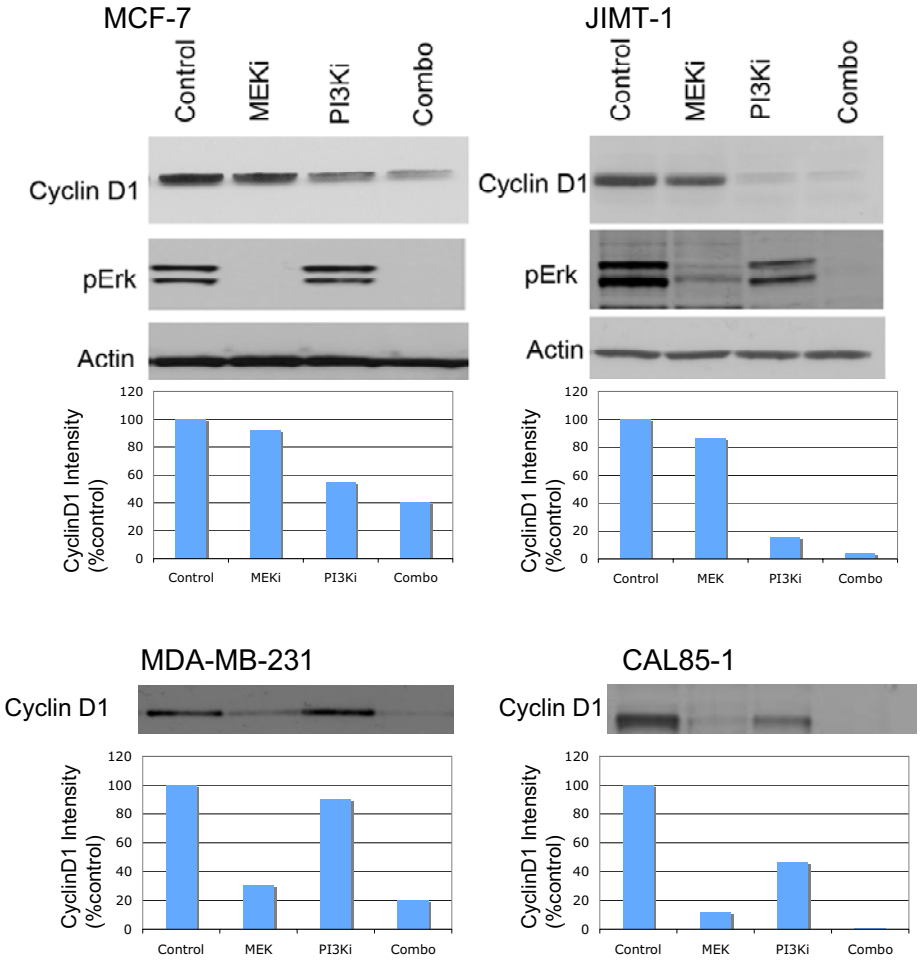

Supplemental figure 10: FACS assay for TUNEL apoptosis marker shows synergistic increases in apoptotic response in basal-like non-BRAF mutant cell lines but not a luminal cell line. Panel A shows raw FACS data from Hs578t cells and panel B quantitation of data for multiple cell lines. Molecular subtypes and key genetic alterations are indicated under the graph.

A

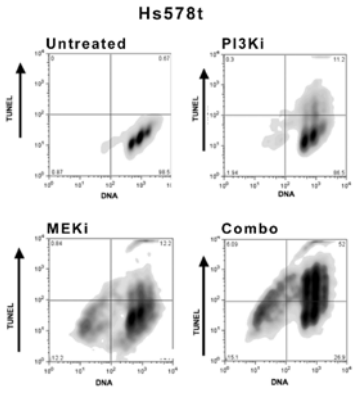

B

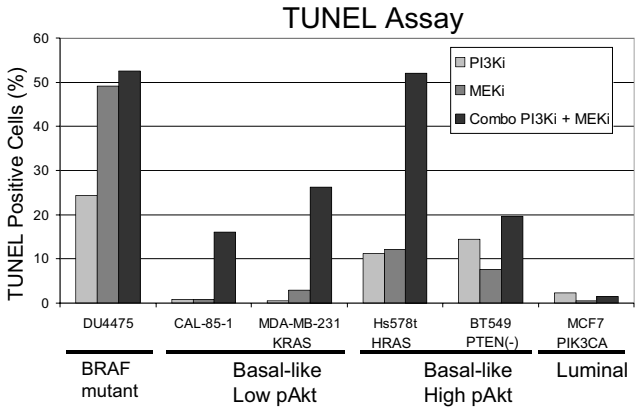

Supplemental figure 11: A MEK and PI3 kinase inhibitor combination regimen is well tolerated in mice harboring MX-1 basal-like PTEN null tumors

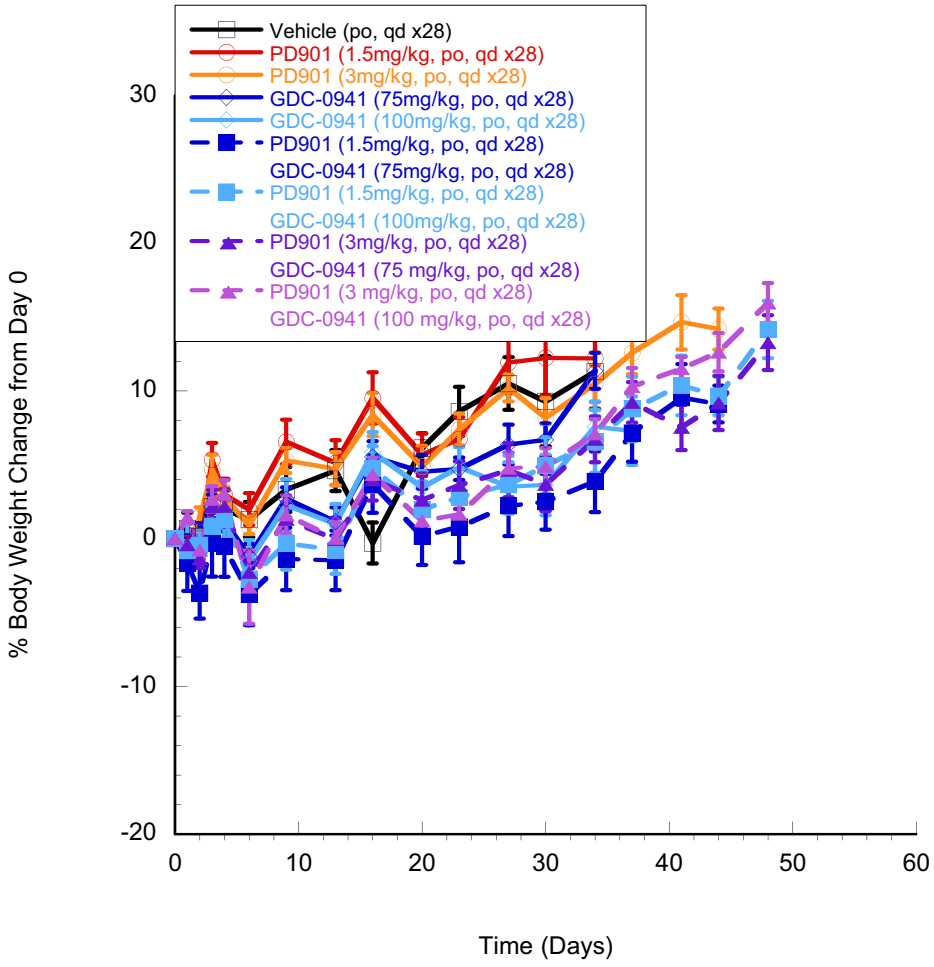

Hoeflich et al Supplemental Materials and Methods:

Cell lines

Breast cancer cell lines AU565, BT-20, BT-474, BT-549, BT-483, CAMA-1, DU4475, HCC1143, HCC1395, HCC1419, HCC1428, HCC1500, HCC1569, HCC1937, HCC1954, HCC2218, HCC38, HCC70, Hs578T, KPL-1, KPL-4, MCF-7, MDA-MB-134-VI, MDA-MB-175-VII, MDA-MB-231, MDA-MB-361, MDA-MB-415, MDA-MB-436, MDA-MB-453, MDA-MB-468, SK-BR-3, SW-527, T-47D, UACC-812, UACC-893, ZR-75-1 and ZR-75-30 were obtained from American Type Culture Collection (ATCC, Manassas, VA). The cell lines CAL-120, CAL-148, CAL-51, CAL-85-1, EFM-19, HDQ-P1, HCC1806, HCC202, EFM-192A, EVSA-T, JIMT-1, and MFM-223 were obtained from the Deutsche Sammlung von Mikroorganismen und Zellkulturen GmbH (DSMZ, Braunschweig, Germany). MX-1 was obtained from the Piedmont Research Center (Wilmington, NC), and BT474M1 is a subclone of BT474 that was obtained from California Pacific Medical Center. All cell lines were maintained in RPMI 1640 or DMEM supplemented with 10% fetal bovine serum (Sigma, St. Louis, MO), non-essential amino acids and 2 mmol/L L-glutamine. The integrity of the cell line panel and confirmation of unique identity all cell lines is of great importance to the conclusions of the study, so we have taken several steps to ensure this integrity. First, all cell lines were newly acquired from the above vendors and characterized and archived at low passage number. As described previously we have profiled the cell lines on Affymetrix 100K mapping SNP arrays (17). SNPs for which no genotype was called in any cell line were excluded. The percentage agreement in genotype at all other SNPs was calculated for each pair of cell lines. The percent agreement values fell clearly into two groups, one around 70% and

one around 99%. Two pairs of cell lines (KPL-1 and MCF-7, AU565 and SKBR3) had percent agreement values above 95% and thus were considered to be of common origin. Otherwise the cell lines used in this study were genetically distinct based on this analysis. In addition, our independent gene expression analyses and classification into molecular subtype for all of the cell lines in the study were compared with the classification described by Neve et al (26) and we found near perfect agreement between the cell lines that overlap between the studies, thus supporting the molecular subtype classification we describe. The one exception is the HCC1500 cell line, which is luminal in our analyses of cells derived from two independent vials ordered from ATCC but is described by Neve et al as basal-like.

High Content Assays for Cell Proliferation

Cells were plated at 5-10K per well (depending on cell line growth properties) in PackardView 96 well plates and allowed to adhere overnight incubating at 37ºC. The following day the cells were treated with the MEK inhibitor and allowed to incubate for 72 hours at 37ºC. BrdU labeling reagent (Cat.# B9285, Sigma) was then added to the cells at a final concentration of 200nM for an additional 5 hours, and then plates were fixed and processed according using the manufacturer's standard protocol. Cells were counterstained with Hoechst-33258 to allow identification of nuclei and the percentage of cells positive for BrdU immunofluorescence was then quantitated for at least 1000 cells per well using Cellomics Target Activation software (www.cellomics.com).

Chou and Talalay combination index experiments

For in vitro combination studies CAL85-1, Hs578t, MCF7 and JIMT-1 cells were plated out in 384 well format and compounds were added in a fixed dose ratio ranging from 1/16 to 8X the EC_{50} of each drug, both alone and in combination. For the MEK inhibitor the range of concentrations spanned 0.04uM to 20μM and for the PI3 Kinase inhibitor the range of concentrations spanned 0.025μM to 13μM.

Protein analyses

For in vitro pharmacodynamic studies, BT474, HDQ-P1, CAL85-1 and MDA-MB-231 cells were plated in 12 well plates and allowed to grow for until cells reached 60-80% confluence. Cells were dosed with 0, 0.1, or 1.0 μM MEK inhibitor and duplicate plates were made for each timepoint. Cells were incubated in the compound for 6 or 24 hours, then washed with cold PBS and processed for Western blotting using standard protocols, as described in the Supplemental Experimental Methods. CAL85-1 cells were cultured in media containing 10 ng/ml EGF to assess pAKT levels since basal levels of pAKT are undetectable in this cell line when cultured in 10% FBS. For analysis of protein expression in tumor xenografts, lysate from tumor samples was collected by adding DNase Lysis Buffer to frozen tissue and pulverized using the TissueLyser (Qiagen, Valencia, CA) as described by the manufacturer.

Primary blotting antibodies used were p27(C-19) (Santa Cruz Biotechnology cat # sc-528), Cyclin D1(DCS-6) (Santa Cruz Biotechnology cat# SC-20044), ERK #9102, pERK (Thr202/Tyr204) (Cell Signaling Technology, cat #9101), Total AKT and pAKT (S473) (Cell Signaling Technology, cat

#9272 and cat #9271). Secondary blotting antibodies used were polyclonal Goat anti-mouse IgG HRP and Polyclonal Goat anti-rabbit IgG HRP (both from Dako, Glostrup, Denmark Cat.# P0161 and P0448, or Cell Signaling Technology Cat. #7076 and #7074).

Quantitative analysis of protein expression using reverse phase protein arrays was performed at Theranostics Health (Rockville, Md) as described previously (Boyd et al., 2008) and in the Supplemental Experimental Procedures.

siRNA Experiments

Transfection efficiency of siRNA was evaluated by qRT-PCR. Optimal siRNA duplex and lipid concentrations were determined for each cell-line. For the adherent cell lines CAL85-1, HDQ-P1, MDA-MB-231 or MDA-MB-436, cells were plated at 6000 cells per well in a 96 well plate with 0.125uL of Lipofectamine RNAiMAX (Cat.#13778-150 Invitrogen, Carlsbad, CA) and 50nM of siRNA per well. Cells were incubated for 3 days in siRNA then the MEK inhibitor was added for 24 hours, followed by addition of CellTiter Glo or processing for Cell Cycle Profiling. For quantitation of siRNA knockdown by PTEN or EGFR duplexes, RNA was collected and isolated using the QIAGEN TurboCapture mRNA Kit (Cat.#72251). cDNA was made using the High Capacity cDNA Revese Transcription Kit (Cat.#4368813) from ABI and qPCR was done using assays on demand from ABI. EGFR(cat.#Hs00193306_m1) and PTEN (cat.#Hs02621230_s1) primer/probe sets were normalized to the average of the housekeeping genes PPIA (cat.#Hs99999904_m1) and UBC (cat.#Hs00824723_m1) and then again to the corresponding NTC siRNA for

each cell line using the ΔΔCT method.

Gene Expression Microarray Analyses

For supervised analysis of breast cancer cell lines, gene expression data were filtered to remove probe sets that showed little variation across the cell lines. Briefly, probes that did not show at least a five fold variation across the samples (max/min>10) and an absolute intensity difference of at least 250 (max-min >250) were excluded from hierarchical clustering analysis. Cell lines were binned into sensitive and resistant classes based on an EC_{50} cutoff of 1μM and the Cyber-T algorithm was implemented to identify genes differentially expressed between the classes. Data preprocessing prior to clustering analysis involved log transforming and median centering gene expression values, after which average linkage clustering was carried out using Spotfire software (www.spotfire.com).

Identification of Activated RAS and MEK signatures

Stocks of recombinant adenoviruses expressing GFP, HRAS (G12V), and MEK1 (S217E S221E) transgenes (henceforth referred to as gain of function constructs, gf) as well as null control vectors, were purchased and propagated in HEK 293 cells according to vendor supplied protocol (Cell BioLabs, San Diego, CA). Viral vectors were isolated and functionally titered using assay kits (Cell BioLabs, San Diego, CA). Optimal multiplicity of infection (MOI) was determined for MCF10A cells by GFP transfection. Cells were then optimally transfected with MEK1, HRAS, and null control vectors. Cells were lysed 24 hours post-transfection with collection of total RNA and protein via a kit (Qiagen, Valencia, CA). Expression upon transfection for MEK1(gf) and HRas(gf) was confirmed by western blot

(data not shown). Isolated RNA was reversed transcribed to cDNA and then run on Human Genome U133P 2.0 Array chips (Affymetrix, Santa Clara, CA). At least five independent replicates were profiled for each expression construct. Differentially expressed genes between cells infected with control vector and MEK(gf) or RAS(gf) vectors were identified by via the Cyber-T algorithm (Baldi and Long, 2001). We developed pathway activation signatures using a variation of the strategy employed by Bild et al (Bild et al., 2006). The positive training data comprised five HRAS and six MEK1 samples, and the negative training data comprised eighteen control samples. The use of test set data when defining metagenes has been shown to improve predictor performance, but has been controversial (Coombes et al., 2007; Potti and Nevins, 2007). We devised an alternative approach to ensure the use of metagenes that would generalize beyond the training set without using test set data. This approach used a large corpus of unrelated microarray data which reflects real and diverse patterns of gene expression. Specifically, microarray data for 9,833 normal tissue samples with HGU133 Plus 2.0 expression data were collected from Gene Logic, Genentech and the Gene Expression Omnibus (GEO) and expression values for each probe were centered about their median. The singular value decomposition of this collection of normal tissue expression data was calculated and the resulting eigenarray matrix was used as a basis for transformation of the training data. The transformed features of the training data were than ordered according to their difference across training set classes by the Rank Product procedure (Breitling et al., 2004). L2 penalized logistic regression models were trained using iteratively re-weighted ridge regression (Park and Hastie, 2008) on the reduced singular value decomposition (West, 2003) of the top N features. The top N features which minimized cross validation error were used to train

the final model. Predicted pathway activation levels derived from the model for each cell line are shown in Supplemental table 1.

Supplemental table 1: Top 100 genes in sensitive vs resistant cell lines

ProbeID	UNQ	UNQ_Short_Name	HUGO Symbol	SRCNAME
227919_at	UNQ28863	YHRL28863	NA	NA
205428_s_at	UNQ9956	CALB2	CALB2	calbindin 2, 29kDa (calretinin)
227458_at	UNQ6713	PDL1/B7-H1	CD274	CD274 molecule
226140_s_at	UNQ16971	OTUD1	OTUD1	OTU domain containing 1
201042_at	UNQ7380	TGM2	TGM2	transglutaminase 2 (C polypeptide, protein-glutamine-gamma-glutamyltransferase)
235911_at	NA	NA	NA	NA
205032_at	UNQ1682	ITGA2	ITGA2	integrin, alpha 2 (CD49B, alpha 2 subunit of VLA-2 receptor)
226757_at	UNQ21425	IFIT2	IFIT2	interferon-induced protein with tetratricopeptide repeats 2
223961_s_at	UNQ5695	CISH	CISH	cytokine inducible SH2-containing protein
227475_at	UNQ24348	FOXQ1	FOXQ1	forkhead box Q1
215543_s_at	UNQ10018	LARGE	LARGE	like-glycosyltransferase
204363_at	UNQ11	TF	F3	coagulation factor III (thromboplastin, tissue factor)
209343_at	UNQ20640	EFHD1	EFHD1	EF-hand domain family, member D1
208250_s_at	UNQ5963	DMBT1	NA	NA
214434_at	UNQ14471	HSPA12A	HSPA12A	heat shock 70kDa protein 12A
203638_s_at	UNQ942	FGFR2	FGFR2	fibroblast growth factor receptor 2 (bacteria-expressed kinase, keratinocyte growth factor receptor, craniofacial dysostosis 1, Crouzon syndror
209011_at	UNQ1870	TRIO	TRIO	triple functional domain (PTPRF interacting)
203896_s_at	UNQ3146	PLCB4	PLCB4	phospholipase C, beta 4
209270_at	UNQ1262	LAMB3	LAMB3	laminin, beta 3
227314_at	UNQ1682	ITGA2	ITGA2	integrin, alpha 2 (CD49B, alpha 2 subunit of VLA-2 receptor)
1555742_at	NA	NA	NA	NA
204508_s_at	UNQ13558	CA12	CA12	carbonic anhydrase XII
201566_x_at	UNQ3216	ID2	ID2	inhibitor of DNA binding 2, dominant negative helix-loop-helix protein
229450_at	UNQ13624	IFIT3	IFIT3	interferon-induced protein with tetratricopeptide repeats 3
213524_s_at	UNQ4406	G0S2	G0S2	G0/G1switch 2
204039_at	UNQ8046	mc/EPB	NA	NA
203963_at	UNQ13558	CA12	CA12	carbonic anhydrase XII
225847_at	UNQ11715	AADACL1	AADACL1	arylacetamide deacetylase-like 1
218086_at	UNQ7114	NPDC1	NPDC1	neural proliferation, differentiation and control, 1
201565_s_at	UNQ3216	ID2	ID2	inhibitor of DNA binding 2, dominant negative helix-loop-helix protein
212148_at	UNQ4995	PBX1	PBX1	pre-B-cell leukemia homeobox 1
214164_x_at	UNQ13558	CA12	CA12	carbonic anhydrase XII
217502_at	UNQ21425	IFIT2	IFIT2	interferon-induced protein with tetratricopeptide repeats 2
204747_at	UNQ13624	IFIT3	IFIT3	interferon-induced protein with tetratricopeptide repeats 3
201095_at	NA	NA	NA	NA
200672_x_at	UNQ7408	SPTBN1	SPTBN1	spectrin, beta, non-erythrocytic 1
218806_s_at	UNQ14258	VAV3	VAV3	vav 3 oncogene
218796_at	UNQ20949	C20orf42	C20orf42	chromosome 20 open reading frame 42
235457_at	UNQ12517	MAML2	NA	NA
201995_at	UNQ5295	EXT1	EXT1	exostoses (multiple) 1
210457_x_at	UNQ5772	HMGA1	HMGA1	high mobility group AT-hook 1
223112_s_at	UNQ14082	NDUFB10	NDUFB10	NADH dehydrogenase (ubiquinone) 1 beta subcomplex, 10, 22kDa
226333_at	UNQ923	IL6R	IL6R	interleukin 6 receptor
60474_at	UNQ20949	C20orf42	C20orf42	chromosome 20 open reading frame 42
206074_s_at	UNQ5772	HMGA1	HMGA1	high mobility group AT-hook 1
218856_at	UNQ437	TNFRSF21	TNFRSF21	tumor necrosis factor receptor superfamily, member 21
224909_s_at	UNQ16674	EAPS16674	NA	NA
209369_at	UNQ14083	ANXA3	ANXA3	annexin A3
227342_s_at	UNQ25939	MYEOV	MYEOV	myeloma overexpressed gene (in a subset of t(11;14) positive multiple myelomas)
215867_x_at	UNQ13558	CA12	CA12	carbonic anhydrase XII
212770_at	UNQ4601	TLE4	TLE3	transducin-like enhancer of split 3 (E(sp1) homolog, Drosophila)
226487_at	UNQ20292	FLJ14721	C12orf34	chromosome 12 open reading frame 34
214581_x_at	UNQ437	TNFRSF21	TNFRSF21	tumor necrosis factor receptor superfamily, member 21
204268_at	UNQ4926	S100A2	S100A2	S100 calcium binding protein A2
230183_at	UNQ5295	EXT1	EXT1	exostoses (multiple) 1
210692_s_at	UNQ32943	SLC43A3	SLC43A3	solute carrier family 43, member 3
1553530_a_at	UNQ1687	ITGB1	ITGB1	integrin, beta 1 (fibronectin receptor, beta polypeptide, antigen CD29 includes MDF2, MSK12)
235106_at	UNQ34598	DHX37	NA	NA
213113_s_at	UNQ32943	SLC43A3	SLC43A3	solute carrier family 43, member 3
217997_at	UNQ7723	PHLDA1	PHLDA1	pleckstrin homology-like domain, family A, member 1
201889_at	UNQ4407	FAM3C	FAM3C	family with sequence similarity 3, member C
213198_at	UNQ917	ACVR1B	ACVR1B	activin A receptor, type IB
219433_at	UNQ16823	BCOR	BCOR	BCL6 co-repressor
227606_s_at	UNQ16509	DNMD16509	STAMBPL1	STAM binding protein-like 1
209946_at	UNQ417	VEGFC	VEGFC	vascular endothelial growth factor C
224925_at	UNQ16674	EAPS16674	NA	NA
212531_at	UNQ1721	LCN2	LCN2	lipocalin 2 (oncogene 24p3)
1553858_at	UNQ11983	ZBTB3	ZBTB3	zinc finger and BTB domain containing 3
212151_at	UNQ4995	PBX1	PBX1	pre-B-cell leukemia homeobox 1
231035_s_at	NA	NA	NA	NA
212071_s_at	UNQ7408	SPTBN1	SPTBN1	spectrin, beta, non-erythrocytic 1
228340_at	UNQ4601	TLE4	TLE3	transducin-like enhancer of split 3 (E(sp1) homolog, Drosophila)
227272_at	UNQ26769	LOC374614	NA	NA
218000_s_at	UNQ7723	PHLDA1	PHLDA1	pleckstrin homology-like domain, family A, member 1
225688_s_at	UNQ20005	PLCXD2	PHLDB2	pleckstrin homology-like domain, family B, member 2
205660_at	UNQ17129	OASL	OASL	2'-5'-oligoadenylate synthetase-like
223194_s_at	UNQ11816	C6orf85	C6orf85	chromosome 6 open reading frame 85
221223_x_at	UNQ5695	CISH	CISH	cytokine inducible SH2-containing protein
223082_at	UNQ16865	SH3KBP1	SH3KBP1	SH3-domain kinase binding protein 1
1553678_a_at	UNQ1687	ITGB1	ITGB1	integrin, beta 1 (fibronectin receptor, beta polypeptide, antigen CD29 includes MDF2, MSK12)
208228_s_at	UNQ942	FGFR2	FGFR2	fibroblast growth factor receptor 2 (bacteria-expressed kinase, keratinocyte growth factor receptor, craniofacial dysostosis 1, Crouzon syndror
223601_at	UNQ20862	OLFM2	OLFM2	olfactomedin 2
209530_at	UNQ2071	CACNB3	CACNB3	calcium channel, voltage-dependent, beta 3 subunit
219014_at	UNQ4513	PLAC8	PLAC8	placenta-specific 8
205490_x_at	NA	NA	NA	NA
211599_x_at	UNQ42	cMet	MET	met proto-oncogene (hepatocyte growth factor receptor)
203108_at	UNQ5187	GPRC5A	GPRC5A	G protein-coupled receptor, family C, group 5, member A
213368_x_at	UNQ14562	PPFIA3	PPFIA3	protein tyrosine phosphatase, receptor type, f polypeptide (PTPRF), interacting protein (liprin), alpha 3
227558_at	UNQ10567	CBX4	CBX4	chromobox homolog 4 (Pc class homolog, Drosophila)
209626_s_at	UNQ14055	OSBPL3	OSBPL3	oxysterol binding protein-like 3
223484_at	UNQ8528	NMES1	C15orf48	chromosome 15 open reading frame 48
1554097_a_at	NA	NA	NA	NA
217999_s_at	UNQ7723	PHLDA1	PHLDA1	pleckstrin homology-like domain, family A, member 1
212143_s_at	UNQ119	IGFBP3	IGFBP3	insulin-like growth factor binding protein 3
221870_at	UNQ20884	EHD2	EHD2	EH-domain containing 2
209012_at	UNQ1870	TRIO	TRIO	triple functional domain (PTPRF interacting)
223301_s_at	UNQ17407	FLJ23518	CCDC82	coiled-coil domain containing 82
223566_s_at	UNQ16823	BCOR	BCOR	BCL6 co-repressor
204011_at	UNQ5147	SPRY2	SPRY2	sprouty homolog 2 (Drosophila)
224583_at	UNQ16648	COTL1	COTL1	coactosin-like 1 (Dictyostelium)

Supplemental table 2: GSEA analysis

p-value	Direction	Number of genes	Gene set Name	Source
1.86E-48	L	465	**Breast cancer_ER_POS Genes whose expression is consistently positively correlated with estrogen recep**	Broad/MIT MSigDB
2.54E-45	U	923	**ras-induced senescent IMR90 fibroblast genes Gene expression changes in ras-induced senescent IMR90**	Mason et al.,Oncogene 23:9238-9246; 2004
1.22E-30	U	314	BREAST CANCER STROMA GENES genes expressed by stroma of GeneLogic human breast cancer samples	Gene logic corporation, Gaithersburg, Md
6.39E-14	U	210	BAF57_BT549_UP Up-regulated following stable re-expression of BAF57 in Bt549 breast cancer cells that lack fu	Broad/MIT MSigDB
4.44E-12	U	123	HCC_SURVIVAL_GOOD_VS_POOR_DN Genes highly expressed in hepatocellular carcinoma with poor survival.	Broad/MIT MSigDB
2.53E-09	U	124	SERUM_FIBROBLAST_CELLCYCLE Cell-cycle dependent genes regulated following exposure to serum in a vari	Broad/MIT MSigDB
2.55E-09	L	50	AGUIRRE_PANCREAS_CHR12 Genes on chromosome 1 with copy-number-driven expression in pancreatic ade	Broad/MIT MSigDB
5.83E-09	U	136	CHANG_SERUM_RESPONSE_UP CSR (Serum Response) signature for activated genes (Stanford)	Broad/MIT MSigDB
8.45E-09	U	46	TGFBETA_EARLY_UP Upregulated by TGF-beta treatment of skin fibroblasts at 30 min (clusters 1-3)	Broad/MIT MSigDB
1.68E-08	U	80	CORDERO_KRAS_KD_VS_CONTROL_UP Genes upregulated in kras knockdown vs control in a human cell line	Broad/MIT MSigDB

Supplemental table 3: Top 50 genes induced by MEK and RAS

ProbeID	t-statistic	pvalue	qvalue	log2(Fold Change)	UNQ	UNQ_Shor	HUGO Symbol	Description
209283_at	-13.469	0	0	-1.472	UNQ2653	CRYAB	CRYAB	crystallin, alpha B
228955_at	9.83	0	0	1.242	UNQ2146	LRP8	LRP8	low density lipoprotein receptor-related protein 8, apolipoprotein e receptor
218856_at	-9.526	0	0	-1.405	UNQ437	TNFRSF21	TNFRSF21	tumor necrosis factor receptor superfamily, member 21
213134_x_	11.135	0	0	0.75	UNQ2194(	BTG3	BTG3	BTG family, member 3
219271_at	10.566	0	0	3.048	UNQ2434	GALNT14	CAPN14|GALNT14	calpain 14|UDP-N-acetyl-alpha-D-galactosamine:polypeptide N-acetylgalactosaminyltransferase 14 (GalNAc-T14)
206114_at	-9.343	0	0	-3.011	UNQ969	EPHA4	EPHA4	EPH receptor A4
202309_at	9.541	0	0	0.881	UNQ3256	MTHFD1	MTHFD1	methylenetetrahydrofolate dehydrogenase (NADP+ dependent) 1, methenyltetrahydrofolate cyclohydrolase, formyl
225520_at	11.123	0	0	1.097	UNQ16577	MTHFD1L	MTHFD1L	methylenetetrahydrofolate dehydrogenase (NADP+ dependent) 1-like
201761_at	13.105	0	0	0.999	UNQ7842	MTHFD2	MTHFD2	methylenetetrahydrofolate dehydrogenase (NADP+ dependent) 2, methenyltetrahydrofolate cyclohydrolase
230266_at	-10.745	0	0	-1.764	UNQ32692	RAB7B	RAB7B	RAB7B, member RAS oncogene family
212190_at	10.41	0	0	1.687	UNQ1485	SERPINE2	SERPINE2	serpin peptidase inhibitor, clade E (nexin, plasminogen activator inhibitor type 1), member 2
209406_at	9.359	0	0	1.052	UNQ17175	BAG2	BAG2	BCL2-associated athanogene 2
200952_s_	-11.504	0	0	-3.501	UNQ2066	CCND2	CCND2	cyclin D2
218585_s_	13.113	0	0	1.22	UNQ14866	DTL	DTL	denticleless homolog (Drosophila)
209800_at	-9.668	0	0	-1.546	UNQ2246(	KRT16	KRT16	keratin 16 (focal non-epidermolytic palmoplantar keratoderma)
205569_at	10.632	0	0	3.735	UNQ12057	LAMP3	LAMP3	lysosomal-associated membrane protein 3
210959_s_	-9.885	0	0	-0.989	UNQ5731	SRD5A1	SRD5A1	steroid-5-alpha-reductase, alpha polypeptide 1 (3-oxo-5 alpha-steroid delta 4-dehydrogenase alpha 1)
205542_at	9.959	0	0	2.085	UNQ9109	STEAP1	STEAP1	six transmembrane epithelial antigen of the prostate 1
223229_at	13.004	0	0	1.304	UNQ10662	UBE2T	UBE2T	ubiquitin-conjugating enzyme E2T (putative)
205393_s_	10.346	0	0	1.109	UNQ5011	CHEK1	CHEK1	CHK1 checkpoint homolog (S. pombe)
201710_at	14.6	0	0	2.559	UNQ2311	MYBL2	MYBL2	v-myb myeloblastosis viral oncogene homolog (avian)-like 2
219493_at	11.655	0	0	1.041	UNQ17150	SHCBP1	SHCBP1	SHC SH2-domain binding protein 1
202589_at	11.505	0	0	1.196	UNQ9766	TYMS	TYMS	thymidylate synthetase
204126_s_	16.226	0	0	4.495	UNQ374	CDC45L	CDC45L	CDC45 cell division cycle 45-like (S. cerevisiae)
224753_at	10.338	0	0	1.597	UNQ16606	CDCA5	CDCA5	cell division cycle associated 5
224428_s_	20.514	0	0	1.723	UNQ12596	CDCA7	CDCA7	cell division cycle associated 7
201710_at	14.6	0	0	2.559	UNQ2311	MYBL2	MYBL2	v-myb myeloblastosis viral oncogene homolog (avian)-like 2
205047_s_	10.67	0	0	2.093	UNQ3246	ASNS	ASNS	asparagine synthetase
205034_at	24.867	0	0	2.722	UNQ10482	CCNE2	CCNE2	cyclin E2
224428_s_	20.514	0	0	1.723	UNQ12596	CDCA7	CDCA7	cell division cycle associated 7
225081_s_	9.781	0	0	0.78	UNQ20685	CDCA7L	CDCA7L	cell division cycle associated 7-like
218741_at	10.134	0	0	1.772	UNQ9633	C22orf18	CENPM	centromere protein M
213008_at	9.988	0	0	1.641	UNQ11516	FKDV1151	FANCI	Fanconi anemia, complementation group I
218350_s_	12.735	0	0	0.882	UNQ9997	GMNN	GMNN	geminin, DNA replication inhibitor
227211_at	9.655	0	0	1.022	UNQ11148	PHF19	PHF19	PHD finger protein 19
219494_at	9.775	0	0	1.38	UNQ16399	RAD54B	RAD54B	RAD54 homolog B (S. cerevisiae)
203968_s_	14.117	0	0	1.779	UNQ14546	CDC6	CDC6	cell division cycle 6 homolog (S. cerevisiae)
202411_at	9.446	0	0	3.95	UNQ5393	IFI27	IFI27|FAM14A	interferon, alpha-inducible protein 27|family with sequence similarity 14, member A
204734_at	-9.46	0	0	-2.46	UNQ7983	KRT19	KRT15|KRT19	keratin 15|keratin 19
213906_at	16.874	0	0	1.787	UNQ5673	MYBL1	MYBL1	v-myb myeloblastosis viral oncogene homolog (avian)-like 1
230356_at	13.106	0	0	1.643	UNQ10354	Sax1	NKX1-2	NK1 homeobox 2
218644_at	9.993	0	0	1.702	UNQ20788	PLEK2	PLEK2	pleckstrin 2
204285_s_	13.816	0	0	1.253	UNQ14985	PMAIP1	PMAIP1	phorbol-12-myristate-13-acetate-induced protein 1
217272_s_	-9.096	0	0	-2.241	UNQ12083	SERPINB1	SERPINB13	serpin peptidase inhibitor, clade B (ovalbumin), member 13
231856_at	12.945	0	0	4.543	UNQ12147	SPQR1214	KIAA1244	KIAA1244
204798_at	9.311	0	0	2.027	UNQ2058	MYB	MYB	v-myb myeloblastosis viral oncogene homolog (avian)
235144_at	16.406	0	0	1.957	UNQ19471	RASEF	RASEF	RAS and EF-hand domain containing
225912_at	-9.259	0	0	-1.617	UNQ21166	TP53INP1	TP53INP1	tumor protein p53 inducible nuclear protein 1
218807_at	-9.498	0	0	-1.125	UNQ14256	VAV3	VAV3	vav 3 guanine nucleotide exchange factor
202095_s_	10.425	0	0	1.59	UNQ6162	BIRC5	BIRC5	baculoviral IAP repeat-containing 5 (survivin)

Supplemental table 4: Ras pathway predictors

Cell Line	mcf10a_RAS MEK predictor
MDA-MB-134VI	1.561522258
HDQ-P1	3.005412519
DU4475	5.088272929
MT-3	0.094212097
HCC1806	6.057952552
MDA-MB-435S	7.897471489
HCC70	5.209717563
HCC1954	7.271376772
CAL-120	7.825616103
MX1	1.526650039
CAL-85-1	5.877978641
SW527	3.000730351
CAL-51	4.83582616
MDA-MB-231	7.812897994
HCC1143	9.828949712
BT-20	-0.715458478
MDA-MB-175-VII	-5.916575386
HS 578T	-0.493018017
MDA-MB-468	8.422287698
HCC1395	-1.454714578
MFM-223	1.755087639
AU565	-0.684587495
BT-474	-0.432212789
BT-483	-3.779623789
BT-549	3.470857318
CAL-148	-4.634639056
CAMA-1	1.063519427
EFM-19	-0.931087696
EFM-192A	0.989251324
EVSA-T	-2.805201836
HCC1187	2.760688293
HCC1419	-5.284668636
HCC1428	-0.996595596
HCC1500	-0.632811063
HCC1569	3.282208361
HCC1937	4.819642478
HCC2218	-10.28517067
HCC38	2.66314843
JIM-T	3.152998211
KPL-1	-6.409216711
KPL4	-2.411538379
MCF7	-5.795687238
MDA-MB-361	-2.048195804
MDA-MB-415	0.793425341
MDA-MB-436	3.041703724
MDA-MB-453	-1.91388501
SK-BR-3	-4.747140587
T-47D	-1.580969544
UACC-812	-3.741796407
UACC-893	-2.44463976
ZR-75-1	-1.924760377
ZR-75-30	-2.646637775